energies

MDPI

Article

Research on Strategies for Air-Source Heat Pump Load Aggregation to Participate in Multi-Scenario Demand Response

Haiping Liang [1], Xin Xie [1,*], Meng Liu [2], Shengsuo Niu [1] and Haifeng Su [1]

[1] Department of Electric Power Engineering, North China Electric Power University, Baoding 071003, China; hfsups@163.com (H.S.)
[2] Electric Power Research Institute of State Grid Shandong Electric Power Company, Jinan 250003, China
* Correspondence: 220212213202@ncepu.edu.cn

Abstract: Air-source heat pumps (ASHPs), functioning as thermally controlled loads, possess significant adjustable capabilities and controllability when aggregated, establishing them as premium resources for demand-response engagement. This paper proposes a control strategy for the aggregation of ASHP loads to participate in demand response across multiple scenarios, framed within a three-tier architecture: electric power system, Load Aggregator (LA), and thermal load. Load Aggregators, considering the user-comfort temperature ranges and the thermal storage characteristics of buildings, aim to minimize heating costs through time-of-use electricity pricing, while assessing the adjustability of the load. Upon receiving control directives from the power system's dispatch department, the strategy allocates load adjustments by considering user comfort and system regulatory needs, thereby addressing issues like aggregated power oscillations and significant rebound loads. The effectiveness of the proposed strategy is corroborated through simulation, demonstrating its potential to enhance demand-response participation and ameliorate associated power stability challenges.

Keywords: air-source heat pump; demand response; model predictive control; adjustable capability; aggregation control

Citation: Liang, H.; Xie, X.; Liu, M.; Niu, S.; Su, H. Research on Strategies for Air-Source Heat Pump Load Aggregation to Participate in Multi-Scenario Demand Response. *Energies* **2024**, *17*, 2471. https://doi.org/10.3390/en17112471

Academic Editor: Fabio Polonara

Received: 16 April 2024
Revised: 12 May 2024
Accepted: 13 May 2024
Published: 22 May 2024

1. Introduction

The integration of renewable energy sources into power systems on a large scale presents a significant challenge due to their output's inherent randomness and volatility, posing risks to the secure operation of electrical grids [1]. The power system consistently faces the dual challenges of ensuring supply and promoting consumption. With conventional generation sources like thermal power becoming increasingly scarce, harnessing the demand side's regulatory capacity has become crucial for maintaining grid stability [2]. The current research on demand-side management primarily focuses on traditional temperature-controlled loads such as air conditioning and water heaters. ASHPs, as an emerging type of temperature-controlled load, offer advantages in energy efficiency, effectiveness, thermal inertia, and pollution-free operation. Their increasing market share in heating solutions marks them as high-quality resources for demand response in power systems [3].

The participation of temperature-controlled loads in demand-response mechanisms can be broadly categorized into two scenarios [4]: price-based mechanisms and incentive-based mechanisms. The former involve indirectly guiding consumer electricity use through pricing strategies to achieve desired power adjustment outcomes. The latter entail direct agreements between consumers and the power system or LA, where consumers adjust their power usage or receive directives from LA during peak shaving or renewable energy integration phases, with corresponding subsidies provided.

Scholars have extensively explored control methods for heat pump loads. Abdul et al. [5] focused on a start–stop control approach that primarily considers temperature setpoints and is widely applied in engineering practices. David et al. [6] introduces an air-conditioning

system control strategy based on model predictive control (MPC), with the optimization goal of minimizing primary energy consumption to enhance the utilization of renewable energy sources. Gabrielle and Li et al. [7,8] both aimed to minimize operational costs by adjusting heat pump power and indoor temperature constraints, shifting loads during high electricity-price periods, without addressing the assessment of load adjustability potential. Li et al. [9] developed an approximate aggregate model for split air conditioners, calculating the steady-state aggregated power of air-conditioning clusters and evaluating their adjustability for control strategy formulation. Wang et al. [10] considered human thermal comfort by establishing a virtual energy storage model based on the thermodynamics of air conditioning to assess the adjustability potential; however, the model did not cover user participation willingness. Wang et al. [11] proposes a central air-conditioning control strategy based on the adjustable margin of elastic temperature to maximize LA profits. The strategy would benefit from further integrating considerations of user thermal comfort and willingness to participate, enhancing its applicability in engineering contexts.

Given the limited capacity of individual ASHPs, direct control by the power system is impractical, necessitating their aggregation. The aggregation of ASHPs unfolds across two tiers: scheduling and control. The scheduling tier is dedicated to the aggregate modeling of numerous temperature-controlled loads to assess their adjustable capabilities; the control tier, on the other hand, focuses on the collective or individual management of these loads. Li et al. [12] developed a temperature-based aggregation model capable of calculating the stable aggregated power of air-conditioning loads to meet the accuracy requirements of dispatch centers and assess their adjustment potential, thus proving its value for practical application. Feng et al. [13] integrated a clustering method aimed at assessing adjustability in a dual-layer air-conditioning modeling, utilizing the potential shutdown times of air conditioners as criteria to achieve minimized control discrepancies. Wang et al. [14] built on thermodynamic and human comfort models to create a virtual energy storage model analyzing aggregated response capabilities, suggesting enhancements through additional consideration of load controllability and user-response tendencies. Control-wise, Lu et al. [15] employed a state queue model to examine the characteristics of aggregated air-conditioning loads, adjusting power via start–stop control. Saeid et al. [16] pioneered a bilinear spatial model for air-conditioner clusters, applying state-space methods for the aggregate modeling of temperature-controlled loads, offering insights into the state changes within similar load groups and aligning with the usage characteristics of extensive temperature-controlled loads. However, simplifying loads to "on" and "off" states does not suit systems incorporating multiple ASHP units, highlighting the need for research into suitable load aggregation models for ASHPs in demand response.

The aggregated control of ASHPs may disrupt load diversity, causing significant rebound values due to unordered load recall behavior, potentially delivering a "secondary shock" to the grid. Zhou et al. [17] proposed modifying traditional temperature-control methods to mitigate aggregated load fluctuations, addressing power-reduction issues encountered when implementing load-reduction temperature-control strategies by adding a portion of the air-conditioning load to offset power decreases, thereby minimizing the loss of response potential. Jiang et al. [18] modeled this phenomenon of power reduction with the goal of optimizing load reduction during the drop, noting that air-conditioning loads can account for up to 50% of the total grid load during summer peaks, where massive power fluctuations could impact grid safety.

Accordingly, this paper leverages the thermodynamic model from Reference [19] to propose a control strategy for ASHP aggregation in multiple demand-response scenarios. In non-regulatory periods, it employs MPC methods, considering building energy storage characteristics and user thermal comfort, coupled with time-of-use electricity pricing to minimize heating costs, and it assesses load adjustability during each control period, providing decision-making foundations for grid control centers and Load Aggregators (LAs). During regulatory periods, it considers user comfort and regulatory instructions to allocate adjustment power to loads, aiming for higher profits, while controlling the

aggregated power during the ASHP load recovery process to suppress large-scale rebound. Finally, the feasibility of the proposed method is validated through simulation examples, showcasing its potential to enhance demand-response participation and grid stability.

2. Air-Source Heat Pump Load Aggregation Management and Control Architecture

The air-source heat pump load aggregation management and control structure is shown in Figure 1.

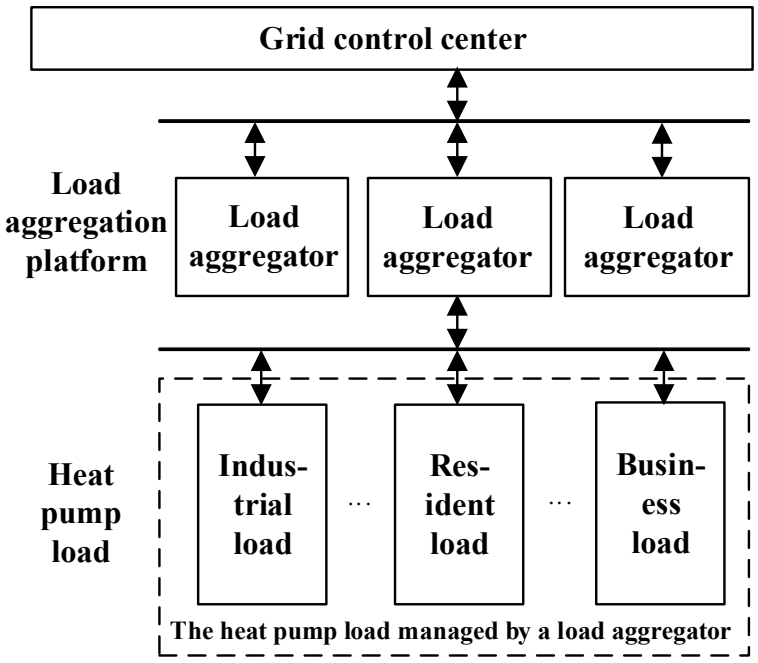

Figure 1. Air-source heat pump load's aggregation control framework.

In the figure, as the highest layer, the grid control center interacts with the LA and issues peak shifting and consumption commands in combination with the load information fed back by the LA to achieve balanced and stable power-system operation. The LA, as the intermediate layer between the grid and the loads, communicates between the grid and the user side, reports the load forecast curves and the adjustable capacity, and provides scheduling-demand information to the control center. The central heating operator of the heat pump load is responsible for the heating business of industrial and commercial buildings and residential users. It can act as a natural LA to build a load-aggregation platform based on its cloud platform and realize load control by combining with the grid regulation and control instructions. As controlled objects, users are the executors of the peaking and consumption tasks.

3. Thermodynamic Modeling of Air-Source Heat Pump Loads

3.1. Analysis of Air-Source Heat Pump Load Operation Mechanism

An air-source heat pump is a device that uses low-level heat energy from the air for heating or cooling, based on the principle of using compressed refrigerant cycles to achieve the transfer of heat energy, as shown in Figure 2.

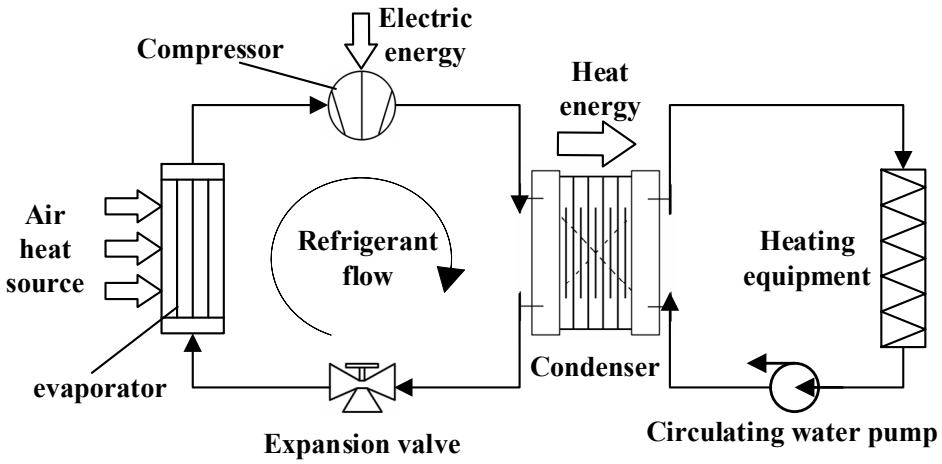

Figure 2. Operating principle of air-source heat pump.

The operation process of an air-source heat pump can be divided into four parts: compression, condensation, expansion, and evaporation. Taking the winter heating state as an example, the refrigerant is compressed into a high-temperature and high-pressure gas in the compressor. It flows into the condenser to exchange heat with the circulating water. This process causes the refrigerant to cool down and transform into a high-pressure liquid. The high-pressure liquid then passes through the expansion valve and enters the evaporator. As the pressure is reduced, the liquid refrigerant evaporates and absorbs heat, reducing the temperature inside the evaporator. Finally, the low-temperature and low-pressure refrigerant undergoes another cycle, constantly absorbing heat in the evaporator and compressor and releasing heat in the condenser. This allows the circulating water to obtain thermal energy, converted into heat energy for the compressor's compression work and obtained from the air. As a result, the air-source heat pump can produce heat energy 4-to-6 times higher than the electrical energy consumption.

The current operation of air-source heat pumps predominantly relies on start–stop control, where they operate at full power during startup and come to a complete stop during shutdown. Typically, a heat pump unit group is formed by parallelly connecting multiple units of the same model. In situations where heat usage is low, only a portion of the heat pumps are activated through control for operation. Moreover, when the indoor temperature fluctuates due to changes in the external environment, the heat pump group can adjust the heat input using start–stop control to maintain a steady indoor temperature. This approach enables precise temperature control, leading to improved energy efficiency and enhanced comfort within the system.

3.2. Air-Source Heat Pump Load Aggregation Model

3.2.1. Heat Pump Unit's Mainframe Model

The energy efficiency ratio of an air-source heat pump represents the ratio of the electrical power input to the compressor to the heating/cooling capacity. The electric–heat relationship for a single unit in heat pump load i can be expressed as follows:

$$Q_{\text{pump},i}(t) = p^{\text{HP}}_{\text{pump},i} \cdot C_{\text{OP},i}(t) \tag{1}$$

$$C_{\text{OP},i} = \frac{T_{\text{out},i}(t)}{T_{\text{out},i}(t) - T_{\text{o}}(t)} \tag{2}$$

where $p^{\text{HP}}_{\text{pump},i}$ is the electric power of a single heat pump in heat pump load i; $Q_{\text{pump},i}$ is the thermal power of a single heat pump in heat pump load i; $C_{\text{OP},i}$ is the energy efficiency ratio of heat pump load i; T_{o} is the ambient temperature; and $T_{\text{out},i}$ is the outlet water temperature of heat pump load i.

The power expression for heat pump load i is

$$Q_i(t) = \sum_{j=1}^{N} C_{\mathrm{OP},i}(t) \cdot S_{i,j}(t) \cdot p_{\mathrm{pump},i}^{\mathrm{HP}} \tag{3}$$

$$u_{\mathrm{pumps},i}^{\mathrm{on}} = \sum_{j=1}^{N} S_{i,j} \tag{4}$$

$$P_i(t) = u_{\mathrm{pumps},i}^{\mathrm{on}}(t) \cdot p_{\mathrm{pump},i}^{\mathrm{HP}} \tag{5}$$

where Q_i is the thermal power of heat pump load i; $u_{\mathrm{pumps},i}^{\mathrm{on}}$ is the number of heat pump load i turned on; $S_{i,j}$ is the switching status of unit j in heat pump load i, which is 1 when it is turned on and 0 when it is turned off; and N is the number of units in heat pump load i.

3.2.2. Heat Pump Water-Cycle Modeling

According to the first law of thermodynamics, the relationship between the temperature of the effluent water from heat pump load i as a function of time, t, is

$$C_{\mathrm{out},i} \frac{\mathrm{d}T_{\mathrm{out},i}}{\mathrm{d}t} = K_{\mathrm{water},i}(T_{\mathrm{re},i} - T_{\mathrm{out},i}) + Q_i \tag{6}$$

where $T_{\mathrm{re},i}$ is the return water temperature of heat pump load i; $C_{\mathrm{out},i}$ is the heat capacity of the outlet water of heat pump load i; and $K_{\mathrm{water},i}$ is the thermal conductivity of the circulating water of heat pump load i.

The variation in the air-source heat pump's return water temperature with time, t, can be expressed as follows:

$$C_{\mathrm{re},i} \frac{\mathrm{d}T_{\mathrm{re},i}}{\mathrm{d}t} = K_{\mathrm{water},i}(T_{\mathrm{out},i} - T_{\mathrm{re},i}) + Q_{\text{room-water},i} \tag{7}$$

where $C_{\mathrm{re},i}$ is the heat capacity of the return water for heat pump load i, and $Q_{\text{room-water},i}$ is the power of heat exchange between the room and the circulating water.

The heat exchange between the circulating water in the end room and the room is expressed as follows:

$$Q_{\text{room-water},i} = K_{\text{room-water},i}(T_{\mathrm{room},i} - T_{\mathrm{out},i}) \tag{8}$$

where $T_{\mathrm{room},i}$ is average room temperature for heat pump load i, and $K_{\text{room-water},i}$ is thermal conductance of the room to the circulating water.

3.2.3. Heat Pump End Heat-Exchange Modeling

The thermal power of the heat pump load is equivalent to the sum of the thermal dynamics of all the rooms. Considering the end as a whole, the heat exchange between the end room and the external environment is expressed as follows:

$$C_{\mathrm{air},i} \frac{\mathrm{d}T_{\mathrm{room},i}}{\mathrm{d}t} = K_{\mathrm{air},i}(T_{\mathrm{o}} - T_{\mathrm{room},i}) - Q_{\text{room-water},i} \tag{9}$$

where $K_{\mathrm{air},i}$ is the thermal conductivity of the end room, and $C_{\mathrm{air},i}$ is the heat capacity of the end room.

4. Optimized Operation Control Methods for Air-Source Heat Pump Loads

4.1. MPC-Based Optimal Operation Control Method for Heat Pump Loads

In practice, LAs sign heating agreements with users and charge residential users for heating based on the area of heating. Therefore, the aggregator needs to minimize the heating cost, while ensuring user comfort in order to maximize benefits. During normal operation, the utilization of heat pump-load thermal energy-storage characteristics,

combined with time-of-use tariffs, allows for the rational scheduling of unit activation and deactivation, resulting in reduced operating costs and smoothed intermittent load fluctuations. This approach also effectively reduces peak-to-valley differences in the power system. This paper adopts the MPC method to achieve the optimal operation of heat pump loads, with the objective of minimizing heating costs. By using rolling optimization instead of one-time global optimization, the optimal operating power for each control cycle is obtained.

4.1.1. Objective Function

The heating cost is taken as the objective function, and its value is the product of the load power and the current electricity price. When the heating demand is met, the size of heating costs is highly correlated with changes in electricity prices.

$$\min F = \sum_{i=1}^{M} \sum_{k=1}^{J} \left\| u_{\text{pumps},i}^{\text{on}}(k) \cdot p_{\text{pump},i}^{\text{HP}} \cdot P_{\text{price}}(k) \cdot T \right\|_2 \tag{10}$$

where $\|\cdot\|_2$ is the 2-Norm, M is the number of heat pump loads in LA, $P_{\text{price}}(k)$ is the tariff for control cycle k, T is the duration of control cycle k, and J is the forecast time domain.

4.1.2. Constraints

(1) Dynamic modeling constraints for heat pump units:

Rewriting Equations (1)–(9) as discrete state equations results in the following:

$$\boldsymbol{X}_i(k+1) = \boldsymbol{A}_i \cdot \boldsymbol{X}_i(k) + \boldsymbol{B}_i \cdot u_{\text{pumps},i}^{\text{on}}(k) + \boldsymbol{D}_i \cdot T_{\text{o}}(k) \tag{11}$$

$$T_{\text{room},i}(k+1) = \begin{bmatrix} 0 & 0 & 1 \end{bmatrix} \cdot \boldsymbol{X}_i(k+1) \tag{12}$$

$$\boldsymbol{A}_i = \begin{bmatrix} 1 - \frac{K_{\text{water},i}}{C_{\text{out},i}} & \frac{K_{\text{water},i}}{C_{\text{out},i}} & 0 \\ \frac{K_{\text{water},i} - K_{\text{room-water},i}}{C_{\text{re},i}} & 1 - \frac{K_{\text{water},i}}{C_{\text{re},i}} & \frac{K_{\text{room-water},i}}{C_{\text{re},i}} \\ \frac{K_{\text{room-water},i}}{C_{\text{air},i}} & 0 & 1 - \frac{K_{\text{air},i} + K_{\text{room-water},i}}{C_{\text{air},i}} \end{bmatrix} \tag{13}$$

$$\boldsymbol{B}_i = \begin{bmatrix} \frac{C_{\text{OP},i}(t) \cdot p_{\text{pump},i}^{\text{HP}}}{C_{\text{out},i}} & 0 & 0 \end{bmatrix}^T \tag{14}$$

$$\boldsymbol{D}_i = \begin{bmatrix} 0 & 0 & \frac{K_{\text{air},i}}{C_{\text{air},i}} \end{bmatrix}^T \tag{15}$$

where $\boldsymbol{X}_i(k)$ is the state vector, $[T_{\text{out},i}(k), T_{\text{re},i}(k), T_{\text{room},i}(k)]^T$, of heat pump load i at control cycle k.

(2) Unit start/stop control constraints

$$u_{\text{pumps},i}^{\min} \le u_{\text{pumps}}^{\text{on}} \le u_{\text{pumps},i}^{\max} \tag{16}$$

where $u_{\text{pumps},i}^{\min}$ is the minimum number of units on for heat pump load i, and $u_{\text{pumps},i}^{\max}$ is the maximum number of units on for heat pump load i.

(3) Indoor temperature constraints

$$T_{\text{room},i}^{\min} \le T_{\text{room},i} \le T_{\text{room},i}^{\max} \tag{17}$$

where $T_{\text{room},i}^{\min}$ is the upper limit of indoor temperature, and $T_{\text{room},i}^{\max}$ is the lower limit of indoor temperature.

The selection of the MPC control period and prediction time domain is crucial for efficient operation. A shorter control period can lead to increased communication difficulty and damage to the unit due to frequent starting and stopping. Conversely, too long of a control interval may result in indoor temperatures exceeding the set upper and lower limits before the subsequent control action is implemented. Furthermore, an excessively

long prediction time domain can impose a higher computational burden and render the situation infeasible. Taking into consideration the ultra-short-term prediction range of the new energy station, which spans from 15 min to 4 h, with a time resolution of 15 min, and in order to accommodate the scale of the power system, this study selects a control period of 15 min and a prediction time domain of four hours. Consequently, Equation (11) is reformulated as follows:

$$\boldsymbol{X}_i(k+T) = \boldsymbol{A}_i' \cdot \boldsymbol{X}_i(k) + \boldsymbol{B}_i' \cdot u_{\text{pumps},i}^{\text{on}}(k) + \boldsymbol{D}_i' \cdot T_{\text{o}}(k) \tag{18}$$

$$\boldsymbol{A}_i' = \boldsymbol{A}_i^{900} \tag{19}$$

$$\boldsymbol{B}_i' = \sum_{z=1}^{899} \boldsymbol{A}_i^z \boldsymbol{B}_i \tag{20}$$

$$\boldsymbol{D}_i' = \sum_{z=1}^{899} \boldsymbol{A}_i^z \boldsymbol{D}_i \tag{21}$$

where $\boldsymbol{A}_i'$, $\boldsymbol{B}_i'$, and $\boldsymbol{D}_i'$ are the thermodynamic parameters of heat pump load i when the control period is 15 min, respectively.

The aggregated power of the heat pump load is

$$P_{\text{agg}}(k) = \sum_{i=1}^{M} P_i(k) \tag{22}$$

where P_{agg} is the heat pump load aggregate power in control period k.

4.2. Methodology for Assessing Adjustable Capacity

The air-source heat pump load aggregation participating in the power system demand response must be assessed for its adjustable capacity. The aggregated power and adjustable capacity of the heat pump are reported to the grid dispatch center as the primary data so that the grid can issue a regulation instruction to the LA in the case of insufficient or excess power, considering various factors. In actual regulation, the grid grants subsidies to LA based on the degree of participation in the demand response. Therefore, improving the adjustable capacity can obtain higher revenue. A heat pump-load adjustable-capacity assessment method is proposed which takes into account the influence of user thermal comfort on adjustable capacity and takes the user thermal-comfort temperature range as the essential adjustable capacity. On this basis, users are divided into two categories according to their willingness to participate in demand response: Class I, during the regulation period, is willing to sacrifice a certain degree of comfort in exchange for a reduction in heating costs by short-term adjustment of the heating temperature range to enhance the adjustable capacity; and Class II is not willing to sacrifice comfort, thus accepting heating costs by the prescribed amount of payment.

The air-source heat pump load's adjustable potential is modeled as follows:

$$u_{\text{pumps},i}^{\text{up}}(k) = {\boldsymbol{B}_{i,3}'}^{-1}(T_{\text{room},i}^{\max}(k) - \boldsymbol{A}_{i,3}' \cdot T_{\text{room},i}(k) - \boldsymbol{D}_{i,3}' \cdot T_{\text{o}}(k)) \tag{23}$$

$$u_{\text{pumps},i}^{\text{down}}(k) = {\boldsymbol{B}_{i,3}'}^{-1}(T_{\text{room},i}^{\min}(k) - \boldsymbol{A}_{i,3}' \cdot T_{\text{room},i}(k) - \boldsymbol{D}_{i,3}' \cdot T_{\text{o}}(k)) \tag{24}$$

where $u_{\text{pumps},i}^{\text{up}}$ and $u_{\text{pumps},i}^{\text{down}}$ are the maximum and minimum number of heat pumps that can be switched on for heat pump load i in control cycle k; and $\boldsymbol{A}_{i,3}'$, $\boldsymbol{B}_{i,3}'$, and $\boldsymbol{D}_{i,3}'$ are the third-row vectors of $\boldsymbol{A}_i'$, $\boldsymbol{B}_i'$, and $\boldsymbol{D}_i'$.

The adjustable capacity of the load is

$$\Delta P_i^{\text{up}}(k) = p_{\text{pump},i}^{\text{HP}} \cdot (u_{\text{pumps},i}^{\text{up}}(k) - u_{\text{pumps},i}^{\text{on}}(k)) \tag{25}$$

$$\Delta P_i^{\text{down}}(k) = p_{\text{pump},i}^{\text{HP}} \cdot (u_{\text{pumps},i}^{\text{down}}(k) - u_{\text{pumps},i}^{\text{on}}(k)) \tag{26}$$

where P_i^{up} and P_i^{down} are the control period k and load i maximum and minimum adjustable power.

As shown in Figure 3, the evaluation of the load adjustability of air-source heat pumps is divided into the following situations:

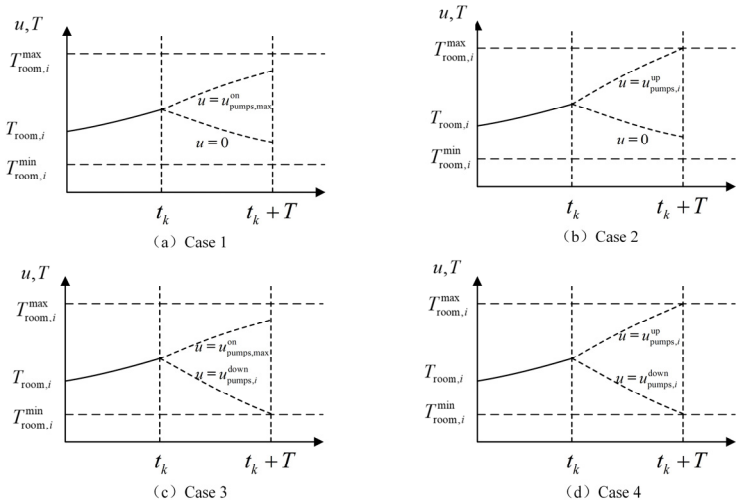

Figure 3. Schematic diagram of adjustability evaluation.

Case 1: $u_{\text{pumps},i}^{\text{up}} \leq u_{\text{pumps,max}}^{\text{on}}$, and $u_{\text{pumps},i}^{\text{down}} \geq 0$. The heat pump load's adjustment capacity is greater than the power sum of the actual installed units, and the solution result of the above model is the actual adjustable capacity.

Case 2: $u_{\text{pumps},i}^{\text{up}} \geq u_{\text{pumps,max}}^{\text{on}}$, and $u_{\text{pumps},i}^{\text{down}} \geq 0$. as $u_{\text{pumps},i}^{\text{up}} = u_{\text{pumps,max}}^{\text{on}}$. The heat pump load's increase capacity is greater than the actual number of units that can be turned on, so the maximum increase capacity is corrected.

Case 3: $u_{\text{pumps},i}^{\text{up}} \leq u_{\text{pumps,max}}^{\text{on}}$, and $u_{\text{pumps},i}^{\text{down}} \leq 0$. as $u_{\text{pumps},i}^{\text{down}} = 0$. The heat pump load's reduction capacity is greater than the actual number of shutdown units, and the maximum reduction capacity is corrected.

Case 4: $u_{\text{pumps},i}^{\text{up}} \leq u_{\text{pumps,max}}^{\text{on}}$, $u_{\text{pumps},i}^{\text{down}} \leq 0$. as $u_{\text{pumps},i}^{\text{up}} = u_{\text{pumps,max}}^{\text{on}}$, and $u_{\text{pumps},i}^{\text{down}} = 0$. The heat pump load's adjustment capability exceeds the maximum value, so we must correct it.

5. Air-Source Heat Pump Load Aggregation Regulation Model

5.1. Optimization and Synergistic Task Assignment for Multiple Heat Pump Loads

When the grid regulation capacity is insufficient and load-side resources are required to participate directly in grid dispatch, the control center issues regulation instructions to the LA based on the load forecast curve and adjustable capacity reported by the LA. The LA withdraws from the optimal operation control and regulates each heat pump's load power, following the grid's demand. The following requirements should be followed when allocating each load regulation power:

(1) Take the two-paradigm minimum of the difference between the regulation power of each regulation period and the load aggregation regulation power as the objective function, and solve the objective function through optimization to finally determine the regulation power of each heat pump load.

(2) When the target regulation power is small, the first consideration is to regulate under the condition of ensuring its thermal comfort: after all the essential regulation capacity of the heat pump load is put into use, change the heating temperature interval of

Class II users to regulate and reduce the impact of the grid regulation on thermal comfort. Therefore, user i's comfort is defined as

$$\lambda_i = \begin{cases} T^{\max}_{\text{room},i} - T_{\text{room},i} & T_{\text{room},i} > T^{\max}_{\text{room},i} \\ 0 & T^{\min}_{\text{room},i} \le T_{\text{room},i} \le T^{\max}_{\text{room},i} \\ T_{\text{room},i} - T^{\min}_{\text{room},i} & T_{\text{room},i} < T^{\min}_{\text{room},i} \end{cases} \tag{27}$$

5.1.1. Objective Function

The objective function can be set as follows:

$$\min F_1 = \sum_{k=1}^{P} \left\| \Delta P_{\text{ref}} - \sum_{i=1}^{M} \Delta P_i \right\|_2 \tag{28}$$

$$\min F_2 = \sum_{k=1}^{P} \sum_{i=1}^{M_2} \lambda_i \tag{29}$$

where ΔP_{ref} is the target regulation power for control cycle k; ΔP_i is the regulation power for heat pump load i; P is the length of LA participation in regulation; and M_2 is the number of class II users, whose value is less than M.

5.1.2. Constraints

(1) Unit group regulation power constraints:

$$\Delta P_i^{\text{down}} \le \Delta P_i \le \Delta P_i^{\text{up}} \tag{30}$$

(2) The dynamic modeling constraints of the heat pump unit are shown in Equation (18).

5.2. Aggregate Regulated Heat Pump-Load Recovery Modeling

When the regulatory target is achieved, the grid control center disengages from the regulating process performed by the LA to allow for the self-restoration of the load. Like decentralized air conditioning, the regulation process may disrupt load diversity, and the uncoordinated load restoration behavior can result in a significant load rebound, leading to excessive deviation between the aggregate power during the period and the reported load curve. This, in turn, causes a "secondary impact" on the power grid, attributable to grid operations. Hence, limiting power peaks during the load recovery process is imperative to ensure a smooth restoration to the normal operating state. At this stage, the target is defined as the minimum recovery time:

$$\min F_1 = T^2_{\text{end}} - T^1_{\text{end}} \tag{31}$$

where T^1_{end} is the moment of the end of grid regulation, and T^2_{end} is the moment of the end of load restoration.

$$P_{\text{grid,min}} \le \sum_{i=1}^{M} P_i \le P_{\text{grid,max}} \tag{32}$$

where $P_{\text{grid,min}}$ and $P_{\text{grid,max}}$ are the maximum and minimum values of aggregated power in the load recovery phase.

Based on the current load operation state, when the power of the load recovery period is the same as the power of the optimized operation period, it can be assumed that the heat pump load has been restored to the ordinary operation state; that is, it exits the load recovery process.

$$P^{\text{MPC}}_{\text{agg}}(T^2_{\text{end}}) = \sum_{i=1}^{M} u^{\text{up}}_{\text{pumps},i}(T^2_{\text{end}}) \cdot p^{\text{HP}}_{\text{pump},i} \tag{33}$$

where $P^{\text{MPC}}_{\text{agg}}$ is the aggregation power during the load recovery stage.

5.3. Solution Method Based on Multi-Objective Atomic Orbit Search Algorithm

The above problem is a multi-objective optimization problem, and the Multi-Objective Atomic Orbital Search (MOAOS) algorithm can be considered for the solution. The MOAOS is a computational technology that combines Atomic Orbital Search (AOS) and multi-objective optimization methods to find the optimal electronic structure of complex molecules [20]. The core idea of this algorithm is to determine the optimal electronic structure of the molecule by optimizing the atomic orbital coefficients to minimize the values of multiple objective functions. The following is a summary of its algorithm flow and key formulas:

(1) Initialization

Initialize the set of candidate solutions (electrons). These candidate solutions are randomly distributed within the decision space and represent possible solutions. For the *j*-th dimension in the *i*-th solution, the initial position, $x_{ij}(0)$, is calculated by the following:

$$x_{ij}(0) = x_{ij\min} + rand(x_{ij\max} - x_{ij\min}) \tag{34}$$

where $x_{ij\min}$ and $x_{ij\max}$ represent the minimum and maximum values of the decision variable, respectively; and rand is a uniformly distributed random vector in the range of [0,1].

(2) Objective function evaluation

Calculate the value of the objective function for each candidate solution, including the evaluation of multiple objective functions, representing the energy levels of the electrons surrounding the nucleus.

(3) Quantum Ladders and Hierarchies

Based on the energy levels of electrons, a virtual hierarchical structure is formed around the nucleus. According to the energy level of the solution, multiple virtual layers are constructed around the nucleus. Solutions with lower energy levels (i.e., better optimization target values) are placed in layers closer to the core, while solutions with higher energy levels are placed in layers that are farther away. This positioning is guided by a Probability Density Function.

(4) Non-dominated sorting and file updating

The non-dominated ranking of candidate solutions is performed to identify a set of non-dominated solutions. Use the archive mechanism to store the non-dominated solutions found so far and maintain the diversity of the solution set.

(5) Grid mechanism

Grid the solution space and manage the distribution of solutions in the archive to enhance solution dispersion and coverage.

(6) Leader selection mechanism

"Leaders" are selected from the archives to guide the search process, with solutions in less crowded areas preferred as leaders.

(7) location update

The electrons' position updates are based on their interactions with photons (energy). Depending on the electron's energy level and the binding energy of its level, the electron can absorb or release energy, thereby updating its position. If the energy level of the electron is higher than the binding energy of the layer ($E_i^k \geq B \cdot E^k$), the electron updates its position through the following formula, indicating energy emission: $X_{i+1}^k = X_i^k + \frac{\alpha_i \cdot (\beta_i \cdot LE_k - \gamma_i \cdot BS_k)}{k}$. If the energy level of the electron is lower than the binding energy of the layer ($E_i^k \leq B \cdot E^k$), the electron passes. The following formula updates the position, representing energy absorption: $X_{i+1}^k = X_i^k + \alpha_i \cdot (\beta_i \cdot LE^k - \gamma_i \cdot BS^k)$, where X_i^k and X_{i+1}^k are the current and future variables of the *i*-th candidate solution in the *k*-th layer; LE^k is the candidate solution with the highest energy level in the *k*-th layer; BS^k is the combined state of the *k*-th layer; and α_i, β_i, and γ_i include randomly generated numbers and vectors, evenly distributed within (0, 1), used to determine the absorbed energy.

(8) Iteration and convergence

The above steps are repeated until a specific stopping condition is met, such as a preset number of iterations, or the quality of the solutions in the archive no longer improves significantly.

(9) Output Pareto front

The algorithm finally outputs an approximate Pareto front, which is composed of non-dominated solutions in the archive and represents the best set of trade-off solutions in a multi-objective optimization problem.

6. Calculated Simulation

6.1. Basic Data

Assume that an LA provides heating for 10 communities, and each community is equipped with 20 air-source heat pumps. The parameter settings are shown in Table 1 [21], and time-of-use electricity prices are shown in Table 2. The heating temperature for residents is set uniformly by the aggregator. The winter heating standard is 16~24 °C. Based on the actual operation scenario, the indoor temperature constraint range is set to 18~24 °C. Community No. 6-10 has a high willingness to participate in demand response. The temperature constraint during power grid regulation is 17~25 °C. The ambient temperature and wind speed settings are shown in Figure 4.

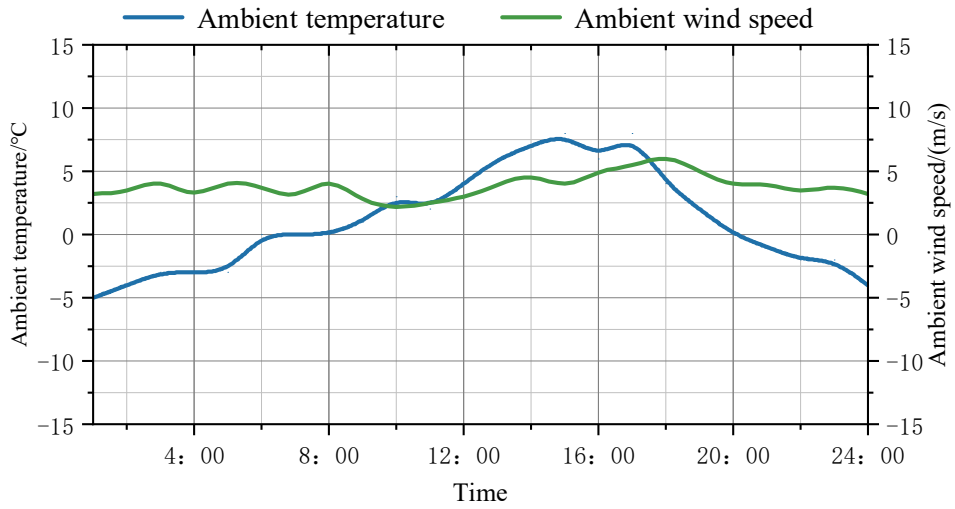

Figure 4. Ambient temperature and ambient wind speed on a typical day in winter.

Table 1. Simulation parameter settings.

Serial Number	Single Heat Pump Power/kW	$C_{out,i}$/J °C^{-1}	$C_{re,i}$/J·°C^{-1}	$C_{air,i}$/J·°C^{-1}	$K_{water,i}$/W·°C^{-1}	$K_{room\text{-}water,i}$/W·°C^{-1}	$K_{air,i}$/W·°C
1	35	6.7×10^7	6.7×10^8	1.5×10^7	2.8×10^5	6.6×10^4	5.2×10^4
2	30	5.8×10^7	4.5×10^8	9.0×10^6	1.4×10^5	3.3×10^4	3.8×10^4
3	35	6.3×10^7	6.2×10^8	1.3×10^7	2.9×10^5	6.6×10^4	5.1×10^4
4	30	4.5×10^7	5.6×10^8	4.2×10^7	2.3×10^5	4.5×10^4	3.3×10^4
5	40	6.7×10^7	6.7×10^8	1.5×10^7	2.8×10^5	6.6×10^4	5.2×10^4
6	35	6.5×10^7	6.6×10^8	1.7×10^7	2.8×10^5	6.4×10^4	5.4×10^4
7	40	7.1×10^7	7.5×10^8	2.1×10^7	3.1×10^5	7.6×10^4	6.4×10^4
8	30	5.4×10^7	4.3×10^8	2.0×10^7	1.9×10^5	7.6×10^4	5.9×10^4
9	45	6.9×10^7	6.5×10^8	1.4×10^7	3.4×10^5	3.6×10^4	5.7×10^4
10	30	4.9×10^7	5.1×10^8	1.5×10^7	5.8×10^5	4.3×10^4	4.1×10^4

Table 2. Time-share tariff.

Period of Time	Electricity Tariff/ USD·kWh^{-1}	Period of Time	Electricity Tariff/ USD·kWh^{-1}
00:00–07:00	0.046	11:00–15:00	0.088
07:00–09:00	0.088	15:00–22:00	0.130
09:00–11:00	0.130	22:00–24:00	0.088

6.2. Analysis of MPC-Based Heat Pump Load Optimization Operation Methods

This article sets the following three strategies for comparison:

Strategy 1: Adopt a start–stop control strategy, turn on the heat pump when the temperature reaches the lower limit, and turn off the heat pump when the temperature reaches the upper limit. The time-of-use electricity price is not considered, and the indoor temperature is set to 18~24 °C.

Strategy 2: Use a constant temperature control strategy to automatically adjust the number of heat pumps to start, regardless of the time-of-use electricity price, and set the indoor temperature to 20 °C.

Strategy 3: Adopt the MPC control strategy, taking into account the time-of-use electricity price, and set the indoor temperature to 18~24 °C.

Under the three strategies discussed, the system's operational costs and energy consumption are illustrated in Table 3. Compared to the first two control strategies, the MPC strategy resulted in a reduction in operational costs by 25.4% and 8.5%, and electricity consumption by 20.2% and 5.9%, respectively. As depicted in Figure 5, when the units are operating normally, the heat pump group adjusts its operational power based on ambient temperature to maintain indoor temperatures at the lower limit, thereby reducing operational costs. Before an increase in electricity prices, non-operating heat pumps are activated to leverage the building's thermal storage characteristics, storing heat in the building in advance; after the price increase, the heat pumps are turned off, relying on the residual heat within the building to meet heating demands. By integrating time-of-use electricity pricing and fully utilizing the building's energy storage features, this strategy achieves a shift in load, significantly lowering the operational costs of the units.

The adjustable capabilities of each control cycle of LA are shown in Figure 6. During periods of stable electricity prices, to minimize heating costs, the number of operational heat pumps is kept to the minimum required for heating comfort, resulting in a higher potential for increasing capacity. Furthermore, as ambient temperature changes, the adjustable power capacity of the heat pump load gradually increases. The aggregated power is lower during the day than at night, thereby further increasing the potential for power augmentation and reducing the potential for power reduction. Groups 6–10, exhibiting higher willingness to adjust their power usage, offer greater adjustable capacity in the same period compared to Groups 1–5. The aggregated power load fluctuates with changes in electricity prices, leading to significant variations in the corresponding adjustable capacity during those periods.

Table 3. Comparison of running results of different strategies.

Strategy	Running Cost/USD	Power Consumption/kWh
1	7115.20	82,491
2	6155.21	72,647
3	5673.94	68,631

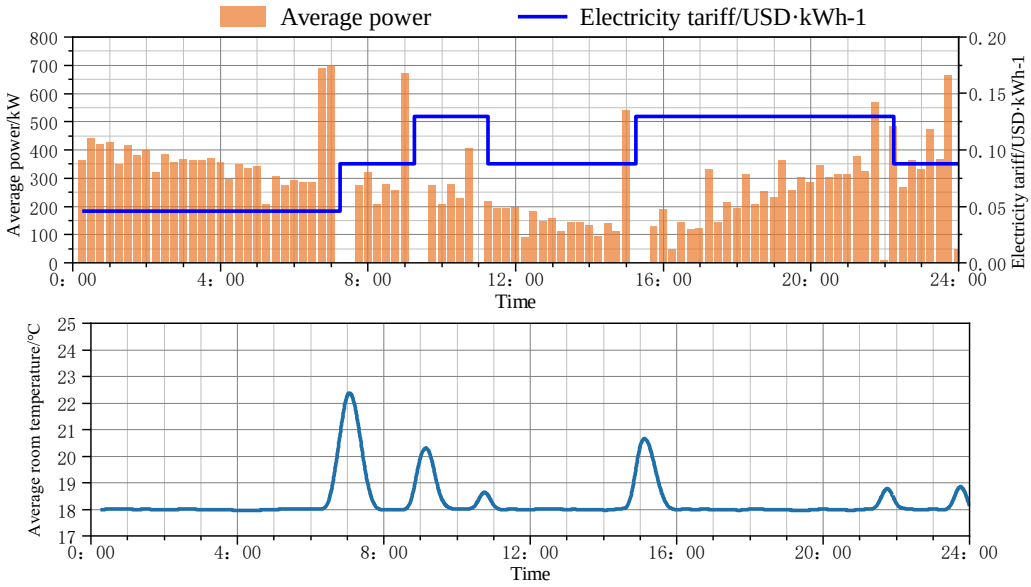

Figure 5. Operation results of heat pump-load optimization.

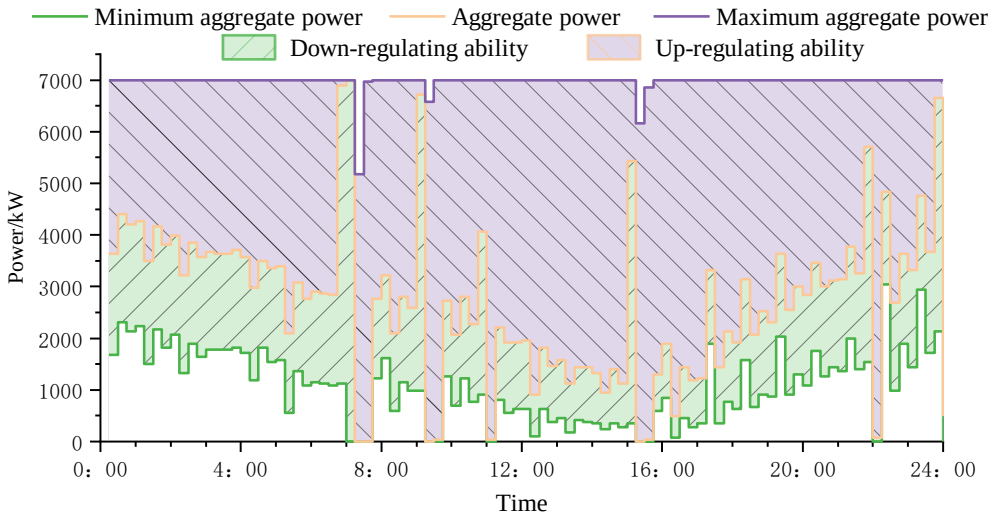

Figure 6. Heat pump load's adjustability.

6.3. Heat Pump Load's Participation in Demand Response and Load Recovery Analysis

Assume that the control center issues control instructions to LA for an increase of 1500 kW, a decrease of 400 kW, and an increase of 1200 kW, respectively, at 4:00–5:00, 12:00–13:00, and 17:00–18:00 on a certain day. The MOAOS algorithm is used to calculate the load output for 500 iterations, so that the aggregate power adjustment amount and user comfort are both optimal.

As shown in Figure 7, when regulation starts, the aggregate power begins to change, and the user's indoor temperature changes, but his/her thermal comfort is not affected. In the power reduction stage at 12:00, the adjustability is low. At this time, only the room temperature of Class II users is lower than 18 °C, but it does not fall below the lower limit of the temperature in the regulation stage.

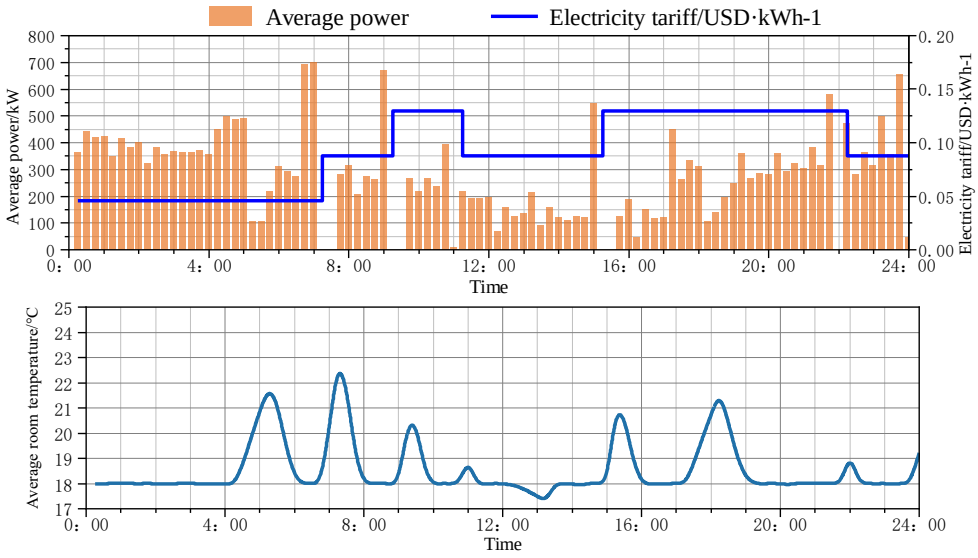

Figure 7. Heat pump-load operation results after grid regulation.

As shown in Figure 8, the adjusted power represents the difference between the actual aggregate power value and the load prediction curve. When the adjusted power is positive, it means that the actual power is greater than the predicted power due to grid regulation. When the adjusted power is negative, it means that the actual power is less than the predicted power. During the grid control period, each control cycle meets the regulation target, and it is also evident that the power rebounds after regulation. This is because, after the end of the grid control, the load enters the MPC optimization operation stage. At this time, the user temperature has ample adjustment space, so many units are adjusted to reduce the heating operation, which causes a "secondary impact" on the power grid. After adopting the power recovery limit, a smooth transition between response and recovery is achieved.

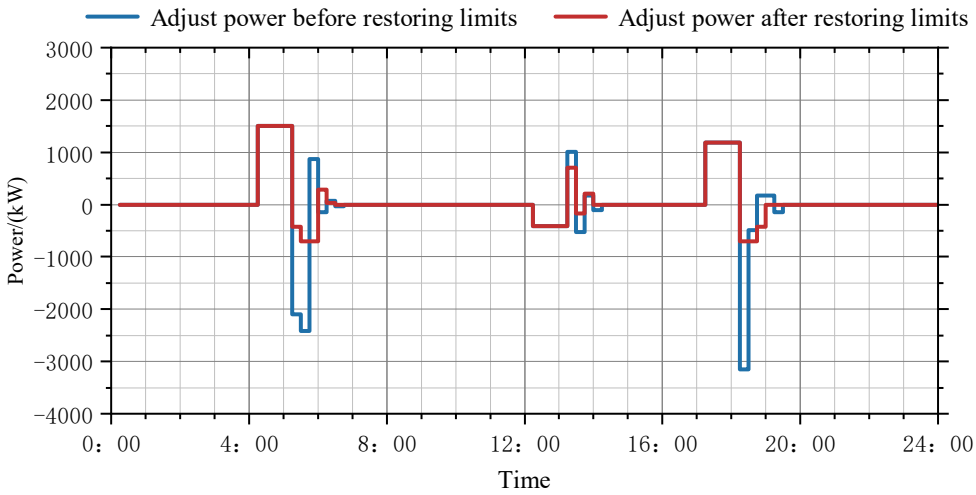

Figure 8. Comparison of adjusted power before and after power restoration limitation.

7. Conclusions

This paper introduces a strategy for aggregating ASHP loads to participate in demand response across multiple scenarios, aimed at enhancing the load-side regulation capability of the electric power system.

(1) During non-regulatory periods of the grid, this approach utilizes MPC methods, taking into account the time-of-use electricity pricing and building thermal-storage characteristics to minimize heating costs for users. This strategy not only improves the load

electricity-consumption profile but also achieves peak shaving and valley filling for the grid. Furthermore, the adjustable capacity of the heat pump loads is assessed during each control period.

(2) In periods when grid regulation is necessary, the strategy adjusts the power output of ASHP loads in response to grid control commands, balancing grid regulatory demands with user comfort. It calculates the power adjustment for each heat pump load, ensuring the smooth recovery of aggregated load power through a minimized recovery time and maximized rebound power control.

Author Contributions: Methodology, H.L. and X.X.; writing—original draft, X.X. and M.L.; writing—review and editing, H.L. and M.L.; data curation, H.S. and S.N. All authors have read and agreed to the published version of the manuscript.

Funding: This research received no external funding.

Data Availability Statement: Data are contained within the article.

Conflicts of Interest: Author Meng Liu was employed by Electric Power Research Institute of State Grid Shandong Electric Power Company. The remaining authors declare that the research was conducted in the absence of any commercial or financial relationships that could be construed as a potential conflict of interest.

References

1. He, G.; Lin, J.; Sifuentes, F.; Liu, X.; Abhyankar, N.; Phadke, A. Rapid cost decrease of renewables and storage accelerates the decarbonization of China's power system. *Nat. Commun.* **2020**, *11*, 2486. [CrossRef] [PubMed]
2. Wang, S.; Li, F.; Zhang, G.; Yin, C. Analysis of energy storage demand for peak shaving and frequency regulation of power systems with high penetration of renewable energy. *Energy* **2023**, *267*, 126586. [CrossRef]
3. Wang, X.; Xia, L.; Bales, C.; Zhang, X.; Copertaro, B.; Pan, S.; Wu, J. A systematic review of recent air source heat pump (ASHP) systems assisted by solar thermal, photovoltaic and photovoltaic/thermal sources. *Renew. Energy* **2020**, *146*, 2472–2487. [CrossRef]
4. Jiang, T.; Li, Y.; Jiang, Y.; Zhou, H.; Ju, P. A review of key technologies for temperature-controlled loads to provide auxiliary services for power systems. *Power Syst. Autom.* **2022**, *46*, 191–207. (In Chinese) [CrossRef]
5. Afram, A.; Janabi-Sharifi, F. Theory and applications of HVAC control systems—A review of model predictive control (MPC). *Build. Environ.* **2014**, *72*, 343–355. [CrossRef]
6. Sturzenegger, D.; Gyalistras, D.; Gwerder, M.; Sagerschnig, C.; Morari, M.; Smith, R. Model Predictive Control of a Swiss office building. *Clima* **2013**, *2013*, 3227–3236. [CrossRef]
7. Masy, G.; Georges, E.; Verhelst, C.; Lemort, V.; André, P. Smart grid energy flexible buildings through the use of heat pumps and building thermal mass as energy storage in the Belgian context. *Sci. Technol. Built Environ.* **2015**, *21*, 800–811. [CrossRef]
8. Li, X.; Malkawi, A. Multi-objective optimization for thermal mass model predictive control in small and medium size commercial buildings under summer weather conditions. *Energy* **2016**, *112*, 1194–1206. [CrossRef]
9. Li, N.; Chu, X.; Zhang, W.; Liu, M. Multiregional air conditioning load aggregation model considering parameter space differences. *J. Electr. Power Syst. Autom.* **2012**, *24*, 19–24. (In Chinese) [CrossRef]
10. Wang, Y.; Tong, Y.; Huang, M.; Yang, L.; Zhao, H. Research on virtual energy storage model of air conditioning load based on demand side response. *Power Grid Technol.* **2017**, *41*, 394–401. (In Chinese) [CrossRef]
11. Wang, D.; Lan, Y.; Jia, H.; Hu, Q.; Yu, J.; Yao, C. Double-layer optimization of central air conditioning cluster demand response based on elastic temperature adjustable margin. *Power Syst. Autom.* **2018**, *42*, 118–126. (In Chinese) [CrossRef]
12. Li, Y.; Yao, J.; Yong, T.; Ju, P.; Yang, S.; Shi, X. Research on evaluation method of aggregate power and response potential of residential temperature-controlled loads. *Chin. J. Electr. Eng.* **2017**, *37*, 5519–5528. (In Chinese) [CrossRef]
13. Feng, X.F.; Lin, G.Y.; Xu, Q.S.; Lu, S.X.; Xie, T.K. Double-layer dynamic optimization dispatching decision method for cluster air-conditioning load. *Electr. Power Autom. Equip.* **2020**, *40*, 29–36. (In Chinese) [CrossRef]
14. Wang, X.Y.; Xu, J.; Liao, S.Y.; Ke, D.P. Flexible load regulation margin evaluation method considering virtual energy storage characteristics. *Huadian Technol.* **2021**, *43*, 37–45. (In Chinese) [CrossRef]
15. Lu, N. An evaluation of the HVAC load potential for providing load balancing service. *IEEE Trans. Smart Grid* **2012**, *3*, 263–1270. [CrossRef]
16. Bashash, S.; Fathy, H.K. Modeling and control of aggregate air conditioning loads for robust renewable power management. *IEEE Trans. Control Syst. Technol.* **2012**, *21*, 1318–1327. [CrossRef]
17. Zhou, L.; Li, Y.; Gao, C. Improvement of temperature adjustment method and control strategy for aggregate air conditioning load. *Chin. J. Electr. Eng.* **2014**, *34*, 5579–5589. (In Chinese) [CrossRef]
18. Jiang, T.Y.; Jv, P.; Wang, C. Air conditioning load aggregation power model considering the randomness of user adjustment behavior. *Power Syst. Autom.* **2020**, *44*, 105–113. (In Chinese) [CrossRef]

19. Liu, M.; Tian, Y.; Cheng, D.; Zhang, Y.; Ding, L. Modelling and control of central air-conditioning loads for power system emergency frequency control. *IET Gener. Transm. Distrib.* **2022**, *16*, 4054–4067. [CrossRef]
20. Azizi, M.; Talatahari, S.; Khodadadi, N.; Sareh, P. Multiobjective atomic orbital search (MOAOS) for global and engineering design optimization. *IEEE Access* **2022**, *10*, 67727–67746. [CrossRef]
21. Cheng, D.Y. Research on Source-Load Collaborative Backup Optimal Configuration Based on Air Conditioning Load Modeling. Ph.D. Thesis, Shandong University, Jinan, China, 2019. (In Chinese)